

Resistively loaded coplanar waveguide for microwave measurements of induced carriers

Cite as: Rev. Sci. Instrum. **93**, 043901 (2022); <https://doi.org/10.1063/5.0085112>

Submitted: 12 January 2022 • Accepted: 28 February 2022 • Published Online: 01 April 2022

 M. L. Freeman,  Tzu-Ming Lu and L. W. Engel



View Online



Export Citation



CrossMark

ARTICLES YOU MAY BE INTERESTED IN

[A qPlus-based scanning probe microscope compatible with optical measurements](#)

Review of Scientific Instruments **93**, 043701 (2022); <https://doi.org/10.1063/5.0082369>

[Laser-frequency stabilization with differential single-beam saturated absorption spectroscopy of \$^4\text{He}\$ atoms](#)

Review of Scientific Instruments **93**, 043001 (2022); <https://doi.org/10.1063/5.0084605>

[Development and integration of photonic Doppler velocimetry as a diagnostic for radiation driven experiments on the Z-machine](#)

Review of Scientific Instruments **93**, 043502 (2022); <https://doi.org/10.1063/5.0084638>



APL Energy
Bridging basic research and innovative technology that will impact the future
Now Open for Submissions

Resistively loaded coplanar waveguide for microwave measurements of induced carriers

Cite as: *Rev. Sci. Instrum.* **93**, 043901 (2022); doi: [10.1063/5.0085112](https://doi.org/10.1063/5.0085112)
Submitted: 12 January 2022 • Accepted: 28 February 2022 •
Published Online: 1 April 2022



View Online



Export Citation



CrossMark

M. L. Freeman,^{1,2,a)}  Tzu-Ming Lu,^{3,4}  and L. W. Engel^{2,a)}

AFFILIATIONS

¹ Physics Department, Florida State University, Tallahassee, Florida 32306, USA

² National High Magnetic Field Laboratory, Tallahassee, Florida 32310, USA

³ Sandia National Laboratories, Albuquerque, New Mexico 87185, USA

⁴ Center for Integrated Nanotechnologies, Sandia National Laboratories, Albuquerque, New Mexico 87123, USA

^{a)} Authors to whom correspondence should be addressed: MatthewLyleFreeman@outlook.com and engel@magnet.fsu.edu.

ABSTRACT

We describe the use of a coplanar waveguide (CPW) whose slots are filled with a resistive film, a resistively loaded CPW (RLCPW), to measure two-dimensional electron systems (2DESs). The RLCPW applied to the sample hosting the 2DES provides a uniform metallic surface serving as a gate to control the areal charge density of the 2DES. As a demonstration of this technique, we present measurements on a Si metal–oxide–semiconductor field-effect transistor and a model that successfully converts microwave transmission coefficients into conductivity of a nearby 2DES capacitively coupled to the RLCPW. We also describe the process of fabricating the highly resistive metal film required for fabrication of the RLCPW.

Published under an exclusive license by AIP Publishing. <https://doi.org/10.1063/5.0085112>

I. INTRODUCTION

Coplanar waveguide (CPW) is a standard and well-characterized type of microwave transmission line which has the advantage of being constructed on a single plane. A CPW, as shown in Figs. 1(a) and 1(b), is constructed from a metal film forming a driven center conductor and broad ground planes separated by slots. Placing a CPW in capacitive or direct contact with a two-dimensional electron system (2DES) allows for broadband measurements of absorption and phase shift due to the 2DES. CPW-based microwave spectroscopy of this sort has been performed on 2DES hosted in semiconductors^{1–5} and on large-area graphene.^{6–8} In these measurements, the transmission through the CPW is particularly sensitive to the conductivity of the 2DES under the slot regions of the CPW.

In studying 2DES, it is often necessary to vary the density of the system by means of biasing a metallic gate. Some semiconductor-hosted 2DES and high quality graphene and transition metal dichalcogenides are not charged by deliberately placed dopants but rely on charge induced by a gate. Such gates, if in

close proximity to the 2DES, create complications for CPW based microwave measurements because a highly conducting gate screens the microwave electric field, reducing the sensitivity to changes in the conductivity of the 2DES. One approach to this problem has been to fabricate gates spaced away from the CPW and the 2DES and biasing these gates with high voltage. This method³ was performed with a front gate, spaced by a vacuum (or air) gap and a thin glass plate above the CPW, as shown in Fig. 1(a), and also with gates on the back side of a semiconductor wafer (far below the CPW in the figure). When the spaced front gate is used, the density in the slots and under the CPW metal is mismatched unless the 2DES is biased precisely relative to the CPW to match the density in the slots; such matching is difficult in practice. Both the back and spaced front gates have a limited range of density tunability, require high bias voltage, and do not work in some samples. Another approach, which uses a highly conductive gate combined with a sensitive density modulation technique to detect cyclotron resonance, is described in Ref. 4.

In this paper, we demonstrate microwave measurements using a resistively loaded CPW (RLCPW), as shown in Figs. 1(c) and 1(d),

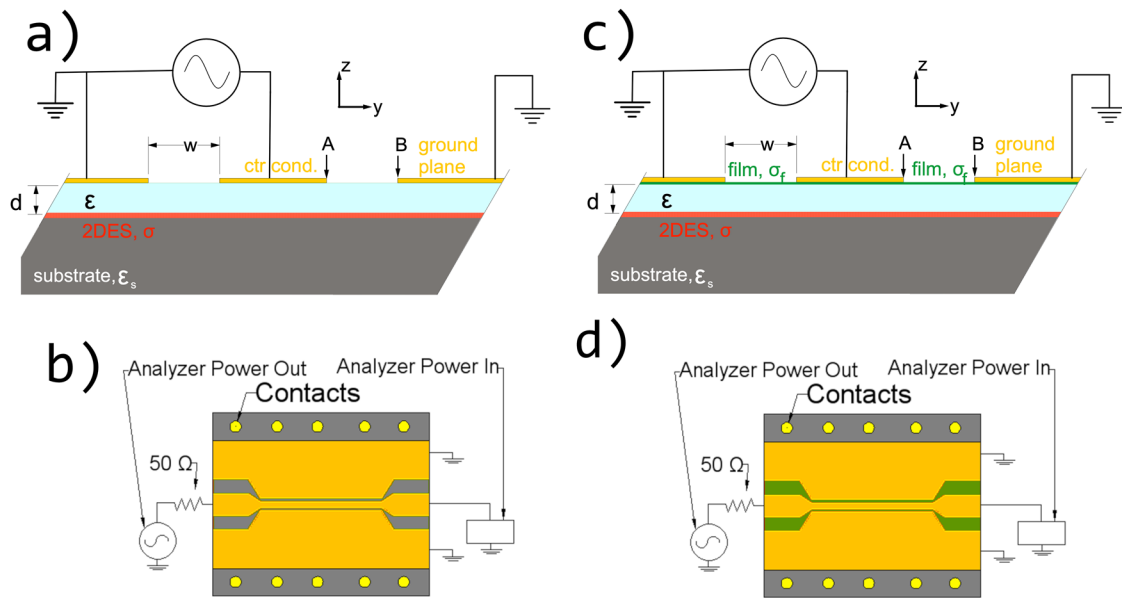


FIG. 1. Coplanar waveguide (CPW) and resistively loaded coplanar waveguide (RLCPW), on top of a two-dimensional electron system (2DES) hosted in a semiconductor. The 2DES is separated from the CPW or RLCPW by a dielectric layer shown as light blue, which has thickness d and dielectric constant ϵ . The highly conductive center conductor and ground planes are shown as gold and the 2DES as red. The slot width is w . In the RLCPW case of (c), the resistive film that bridges the RLCPW slots is shown as green. (a) CPW in cross section. (b) Schematic of CPW in top view. (c) and (d) RLCPW schematics in cross section and top view, respectively. The model in the text refers to points A and B, which mark the edges of the center conductor and side plane at the slot.

in which a resistive film gate is placed under the highly conductive CPW conductors and only partly screens the microwave field. This is analogous to the use of semitransparent gates in optical experiments. Our motivation for this is experimentation in heterojunction insulated gate field effect transistors (HIGFETs),^{9–13} which are semiconductor devices known to give particularly low disorder and wide density tunability. However, for the proof-of-concept demonstration, in this paper, we present data on a Si metal–oxide–semiconductor field-effect transistor (MOSFET), a well-understood device whose large disorder is expected to render its conductivity nearly independent of frequency in our measuring range.

The RLCPW retains the advantages of wide bandwidth and coplanar (single-surface) construction but presents a uniform surface to the sample. In semiconductors, this removes the density gradient due to Schottky potentials and reduces strain due to differential contraction relative to a conventional CPW. Microwave measurements can couple capacitively to samples, so in that case, are essentially contactless, although a single contact to a sample (possibly only at elevated temperature) is required to induce the carriers. The contact, which can be challenging in undoped devices, can be highly resistive, with a leak of $10^{12} \Omega$ or more sufficient to populate most samples. A limitation of the RLCPW measurement is that it becomes insensitive if the 2DES conductivity is much less than that of the resistive film, so fabricating a high resistivity film in the RLCPW is an important aspect of the design. In the following, we describe fabrication and measurement of an RLCPW with a high resistivity metal film on the Si MOSFET. In addition, we present an analytical model for conversion of microwave transmission

measurement to a 2DES conductivity for the capacitively coupled case and compare its results to the measurements.

II. EXPERIMENT SETUP AND MOSFET DEVICE

Figure 1(d) shows a schematic of the experiment with a top view of the RLCPW, which we fabricated as a gate on a MOSFET with an oxide thickness of 35 nm. The edges of the RLCPW are tapered to facilitate a low-reflectance connection to microstrip lines on a kapton film, which are in turn connected to coaxial cables. The length of the RLCPW between the tapers is 2.5 mm, the center conductor width is $45 \mu\text{m}$, and the slot width (w) is $30 \mu\text{m}$. The sample is located in a 0.3 K cryostat and is connected to a room-temperature network analyzer, which serves as a transmitter and receiver. Ohmic contacts on the device enable dc measurements of the MOSFET and allow the 2D channel to be populated by the gate.

For the purpose of charging the channel, the RLCPW can be regarded as a uniform gate. (The microwave voltage applied between the RLCPW center line and its ground planes is much smaller than the dc bias voltages.) For convenience of the microwave connections, the RLCPW is grounded to the cryostat, and we apply negative bias ($-V_b$) to the contacts of the MOSFET relative to that ground to populate the channel. The device substrate is lightly p-type doped with a room temperature resistivity of $1\text{--}10 \Omega \text{ cm}$. This lightly doped substrate freezes out at low temperatures and minimizes microwave absorption at our measuring temperature of 0.3 K. The properties of the oxide layer of the MOSFET are important for the model calculation of conductivity from microwave absorption: the MOSFET

had an oxide thickness of 35 nm and we took the oxide dielectric constant to be 3.7.

A. Resistive film

A key component of the RLCPW is the resistive film. Here, we used a recently developed thin film composed of evaporated Ge, Ni, and Pt layers.¹⁴ The thicknesses of the Ge, Ni, and Pt layers were 20, 0.5, and 1 nm, respectively. After deposition, the film was annealed in a forming gas environment at 525 C for 10 s. This thermal treatment created a resistive film with a resistivity on the order of 1–10 k Ω /sq.¹⁴ In this work, we obtained the 2D resistivity of the film, $\rho_f \approx 3390 \Omega/\text{sq}$, from the dc resistance between the center conductor and the ground planes, making use of the much higher conductivity of the side planes and center conductor.

III. EXPERIMENTAL RESULTS

Using the ohmic contacts, we characterize the MOSFET by standard techniques of dc transport for different V_b as magnetic field (B) is varied. Figure 2(a) shows the diagonal and Hall resistances, R_{xx} and R_{xy} vs B , for several bias voltages. As V_b is increased, R_{xx} decreases and the slope of the Hall resistance decreases due

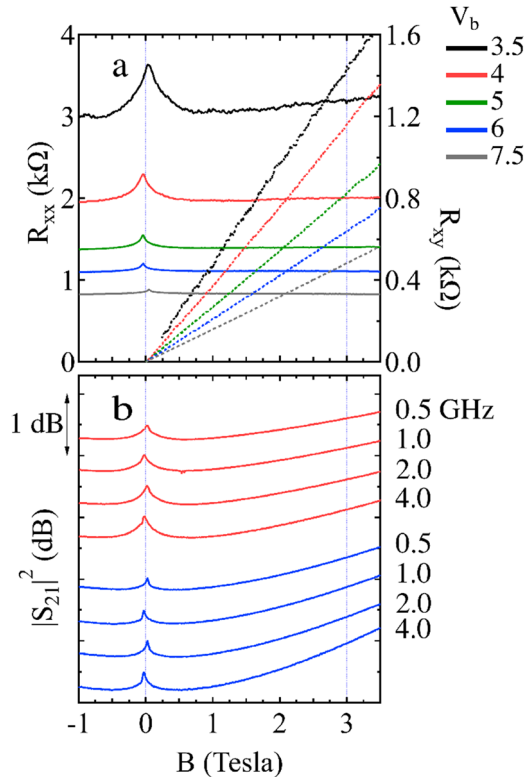


FIG. 2. Field dependence at various gate bias voltages, V_b . (a) DC resistances vs magnetic field. Solid lines are longitudinal resistance R_{xx} (k Ω), and dashed lines are Hall resistance R_{xy} (k Ω). (b) Transmission coefficient $|S_{21}|^2$ (dB) vs magnetic field at various frequencies. The upper (red) group of curves is for $V_b = 4$ V and the lower (blue) is for $V_b = 6$ V. The curves are offset vertically for clarity.

to increasing 2D density, n [shown below in Fig. 4(a)]. The Hall resistance follows the classical formula $R_{xy} = B/ne$. Prominent in these and subsequent traces vs magnetic field is a peak at $B = 0$ due to weak localization; the apparent slight displacement of this peak from $B = 0$ in some traces is an artifact of the remanent field in the superconducting magnet.

Figure 2(b) shows the microwave transmission $|s_{21}|^2$ at various frequencies (f), for $V_b = 4$ and 6 V. Unlike the dc R_{xx} curves of panel (a), the curves exhibit an upward curvature, which arises because the transmission is sensitive to σ_{xx} rather than R_{xx} . The $|s_{21}|^2$ traces are offset from each other for clarity, and their B dependence changes little for the different frequencies. Measurements with long thin transmission lines are nearly insensitive to σ_{xy} , as has been shown for measurements in the quantum Hall regime.¹

IV. ANALYTICAL MODEL

The model presented here can be used to calculate complex transmission coefficient s_{21} ¹⁵ from a 2DES conductivity, given the dimensions of the RLCPW, the film resistivity, and the per unit area capacitance between the 2DES and the film. To convert measured s_{21} to 2DES conductivity, the model must be inverted, which is conveniently done numerically. A more time-consuming alternative to the model is to use commercially available simulator software, such as Sonnet,¹⁶ which we used to check the analytical model.

Figure 1(b) shows a schematic cross section of the RLCPW system narrowly spaced above a 2DES. We model the system in the quasi-TEM approximation, which is applicable to situations where the wavelength is much larger than the RLCPW slot width. Besides high frequency effects, which become important when the wavelength approaches w , the model neglects edge effects¹⁷ and also the capacitance due to lines of force, which terminate at both ends on the 2DES; both these effects are small for the RLCPW with achievable film resistivities. For $w \gg d$, even with the smallest achievable film conductivity σ_f , these effects are not important. Quantum (density of states) capacitance¹⁸ is neglected in this paper and is not important for the MOSFET device but could be incorporated in the coupling capacitance when appropriate.

We consider a distributed circuit, composed of parallel plate transmission lines comprised of the 2DES and the metal above; this approach has been used elsewhere.^{19,20} In the present case, the parallel plate lines are transverse (y direction in Fig. 1) to the RLCPW propagation direction (x in the figure, pointing toward the viewer of the figure) of the RLCPW. The parallel plate lines, whose top layer is the RLCPW and whose bottom layer is the 2DES, have voltage and current related by

$$\begin{aligned} V'_1 &= -Z_1 I_1, & V'_2 &= -\sigma^{-1} I_1, & I'_1 &= (V_2 - V_1) i \omega C_c, \\ I'_2 &= (V_1 - V_2) i \omega C_c, \end{aligned} \quad (1)$$

where primes indicate differentiation in y . V_1, I_1 pertain to the top layer RLCPW and V_2, I_2 to the 2DES. C_c is the capacitance per unit area of the dielectric layer, given by $C_c = \epsilon/d$, where d is the dielectric thickness. Z_1 is taken to be zero for the highly conductive center conductor and side planes and σ_f^{-1} for the region of the slots.

We calculate the complex transmission coefficient s_{21} ¹⁵ using the circuit of Fig. 3 to obtain the load admittance Y_L per unit length

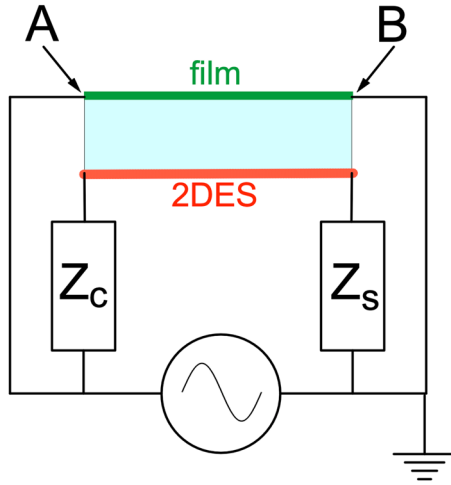


FIG. 3. Circuit model, with Z_c the impedance from the center conductor coupled to the 2DES and Z_s the impedance from the side plane to the 2DES. A and B are the same points as in Fig. 1. Z_c and Z_s are per unit length in the propagation direction, and the 2DES and film are coupled capacitively.

in the propagation direction, presented to the RLCPW by the resistive film and by the capacitively coupled 2DES. In the figure, the impedances $Z_s = (1/i\sigma\omega C_c)^{1/2}$ and $Z_c = Z_s \coth[(i\omega C_c/\sigma)^{1/2}a/2]$ result from Eq. (1) applied to a side plane and the center conductor regions. The resistive film and 2DES couple is between the points marked A and B in the figure. Here, Z_s is taken for a wide side plane, assuming that the current vanishes within the ground plane as y gets farther from the outer edge of the slot, and would need to be modified to include the outside boundary of the side plane in the case^{19,20} of low loss and large kinetic inductance,

$$\begin{bmatrix} 1 \\ 0 \\ 0 \\ 0 \end{bmatrix} = \begin{bmatrix} 0 & 1/2 & \alpha/2 & \alpha/2 \\ Z_c\sigma & 0 & Z_c + 2\beta & Z_c - 2\beta \\ e^{-\gamma w} w & e^{-\gamma w} & -e^{-2\gamma w} \alpha & \alpha \\ e^{-\gamma w} Z_s\sigma & 0 & e^{-2\gamma w} (Z_s - 2\beta) & Z_s + 2\beta \end{bmatrix} \begin{bmatrix} c_1 \\ c_2 \\ c_3 \\ c_4 \end{bmatrix} \quad (2)$$

with $\bar{Z} = (\sigma_f^{-1} + \sigma^{-1})/2$, $\gamma = (2i\omega C_c \bar{Z})^{1/2}$, $\beta = \bar{Z}/\gamma$, and $\alpha = (\gamma\sigma_f)^{-1}$. Of the coefficients c_k , obtained from solving this system, only c_1 is of interest and gives the admittance due to the sample layer, per unit length in the propagation direction of the RLCPW, as $Y_L = -c_1(\sigma_f + \sigma)$.

We design the RLCPW in the quasi-TEM approximation such that if the sample layer and the resistive film were absent, the underlying CPW with characteristic impedance $Z_0 = 50 \Omega$ and phase velocity v_{p0} would result.²¹ (Presently, this task can easily be performed for a substrate of known dielectric constant using online calculators.²²) The model for the RLCPW incorporates Y_L into the admittance per unit length in the propagation direction resulting in propagation constant $\Gamma_R = [i\omega(i\omega + Y_L Z_0 v_{p0})]^{1/2}/v_{p0}$ and characteristic impedance $z_R = (1 - iY_L Z_0 v_{p0}/\omega)^{-1/2}$. z_R is normalized for a

50 Ω measuring system, in which the complex transmission coefficient of the RLCPW is

$$s_{21} = \frac{z_R}{(z_R^2 + 1) \cosh(\Gamma_R l) + 2z_R \sinh(\Gamma_R l)}. \quad (3)$$

V. MICROWAVE CONDUCTIVITY MEASUREMENT WITH THE RLCPW

We demonstrate microwave conductivity measurement with the RLCPW by comparing microwave and dc conductivities, relying on the independence of the conductivity of the MOSFET on the frequency. The disorder in the MOSFET leads to a short carrier momentum relaxation time, τ . Frequency independence is expected when $2\pi f\tau \ll 1$. Using $\tau \sim \sigma_{xx} m^*/ne^2$, where σ_{xx} is taken at zero frequency and field, and for Si the relevant effective mass $m^* \sim 0.19$ free electron masses,²³ we find $\tau \lesssim 2.2 \times 10^{-13}$ s. Hence, $\omega\tau \ll 1$ is satisfied for our measuring conditions ($f \leq 4$ GHz).

We use the dc data of Fig. 2(a) to test obtaining the 2DES conductivity σ_{xx} from microwave measurements. The dc resistivity, ρ_{xx} , is calculated by the van der Pauw method²⁴ from resistances obtained from different sets of ohmic contacts at the edges of the RLCPW. We find the dc σ_{xx} from the tensor inversion, $\sigma_{xx} = \rho_{xx}/(\rho_{xx}^2 + \rho_{xy}^2)$, where the part of R_{xy} that is antisymmetric about $B = 0$ is ρ_{xy} .

Figure 4(b) shows real diagonal conductivities $\text{Re}(\sigma_{xx})$, vs V_b , obtained from dc measurements through the contacts and from

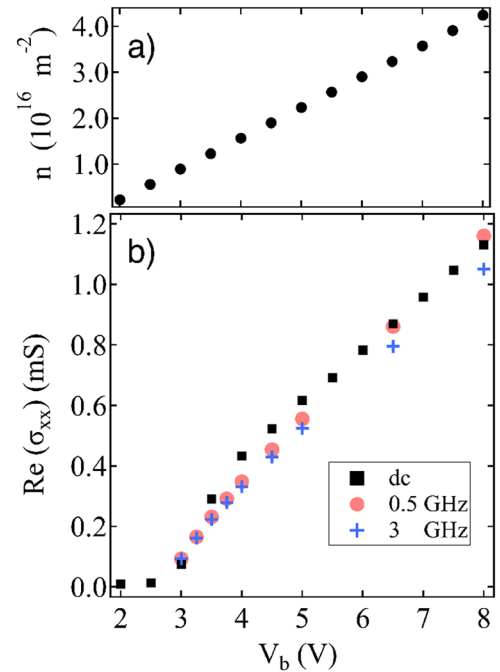


FIG. 4. (a) MOSFET areal density, n , vs bias voltage, V_b . (b) Real diagonal conductivity of the MOSFET, $\text{Re}(\sigma_{xx})$, vs V_b measured at dc and calculated by means of the model (see the text) from normalized $|s_{21}|^2$ at 0.5 and 3 GHz.

s_{21} measurements at frequencies of 0.5 and 3 GHz. To avoid the sharp $B = 0$ weak localization feature in the conductivity, the data were taken with a 2 T magnetic field. To remove the frequency dependent effects of cables, the 0.5 and 3 GHz $\text{Re}(\sigma_{xx})$ data shown were obtained using a simplified calibration procedure, assuming zero absorption from the 2DES at zero bias. We measured $s_{21}(V_b)/s_{21}(V_b = 0)$ and iteratively compared it to the results of the model discussed in Sec. IV for varying σ , $s_{21}(\sigma)/s_{21}(\sigma = 0)$, taking the imaginary part of σ to be zero, as is appropriate for $2\pi f\tau \ll 1$. The dc and microwave $\text{Re}(\sigma_{xx})$ data are grouped together, demonstrating our main point that the RLCPW method can be used to obtain σ_{xx} with appropriate modeling. There are several sources of discrepancies between the points of the three traces on the graph. First, dc resistivity measurements used to calculate $\text{Re}(\sigma_{xx})$ probe different areas on the MOSFET than the RLCPW measurement, which reports conductivity as an average mainly from the areas under the RLCPW slots. The differences between the two microwave frequency data at larger $\text{Re}(\sigma_{xx})$ may be due to the increase in reflection from the RLCPW, which is not removed by the simple calibration procedure.

In summary, we have demonstrated that microwave-frequency measurements can be carried out with an RLCPW transmission line as a sample is gated with a resistive film to vary induced carrier density widely. We have shown that the conductivity of the gated 2DES can be obtained quantitatively from such measurements by means of an analytic model into which the resistivity of the film loading the RLCPW is incorporated.

ACKNOWLEDGMENTS

The microwave measurements and sample design at NHMFL were supported by the Department of Energy (Grant No. DE-FG02-05-ER46212). The National High Magnetic Field Laboratory is supported by the National Science Foundation Cooperative Agreement No. DMR-1644779 and the State of Florida. This work was partly funded by the U.S. Department of Energy (DOE), Office of Basic Energy Sciences (BESs). This work was performed, in part, at the Center for Integrated Nanotechnologies, a U.S. DOE, Office of BESs, user facility. Sandia National Laboratories is a multimission laboratory managed and operated by National Technology and Engineering Solutions of Sandia LLC, a wholly owned subsidiary of Honeywell International, Inc. for the U.S. DOE's National Nuclear Security Administration under Contract No. DE-NA0003525. This paper describes objective technical results and analysis. Any subjective views or opinions that might be expressed in the paper do not necessarily represent the views of the U.S. DOE or the United States Government.

AUTHOR DECLARATIONS

Conflict of Interest

The authors have no conflicts to disclose.

DATA AVAILABILITY

The data that support the findings of this study are available from the corresponding authors upon reasonable request.

REFERENCES

- 1 L. W. Engel, D. Shahar, Ç. Kurdak, and D. C. Tsui, "Microwave frequency dependence of integer quantum Hall effect: Evidence for finite-frequency scaling," *Phys. Rev. Lett.* **71**, 2638–2641 (1993).
- 2 G. Sambandamurthy, Z. Wang, R. M. Lewis, Y. P. Chen, L. W. Engel, D. C. Tsui, L. N. Pfeiffer, and K. W. West, "Pinning mode resonances of new phases of 2D electron systems in high magnetic fields," *Solid State Commun.* **140**, 100–106 (2006).
- 3 A. T. Hatke, Y. Liu, L. W. Engel, M. Shayegan, L. N. Pfeiffer, K. W. West, and K. W. Baldwin, "Microwave spectroscopic studies of the bilayer electron solid states at low Landau filling in a wide quantum well," *Nat. Commun.* **6**, 7071 (2015).
- 4 K. Stone, R. R. Du, M. J. Manfra, L. N. Pfeiffer, and K. W. West, "Millimeter wave transmission spectroscopy of gated two-dimensional hole systems," *Appl. Phys. Lett.* **100**, 192104 (2012).
- 5 I. L. Drichko, A. M. Diakonov, V. A. Malyshev, I. Y. Smirnov, Y. M. Galperin, N. D. Ilyinskaya, A. A. Usikova, M. Kummer, and H. von Känel, "Contactless measurement of alternating current conductance in quantum Hall structures," *J. Appl. Phys.* **116**, 154309 (2014).
- 6 M. Dragoman, D. Neculoiu, A. Cismaru, A. A. Muller, G. Deligeorgis, G. Konstantinidis, D. Dragoman, and R. Plana, "Coplanar waveguide on graphene in the range 40 MHz–110 GHz," *Appl. Phys. Lett.* **99**, 033112 (2011).
- 7 H. S. Skulason, H. V. Nguyen, A. Guermoune, M. Sijak, C. Caloz, and T. Szkopek, "Contactless impedance measurement of large-area high-quality graphene," in *2012 IEEE/MTT-S International Microwave Symposium Digest* (IEEE, 2012), pp. 1–3.
- 8 Y. Wu, Y. Wu, K. Kang, Y. Chen, Y. Li, T. Chen, and Y. Xu, "Characterization of CVD graphene permittivity and conductivity in micro-/millimeter wave frequency range," *AIP Adv.* **6**, 095014 (2016).
- 9 B. E. Kane, L. N. Pfeiffer, and K. W. West, "High mobility GaAs heterostructure field effect transistor for nanofabrication in which dopant induced disorder is eliminated," *Appl. Phys. Lett.* **67**, 1262–1264 (1995).
- 10 R. L. Willett, M. J. Manfra, L. N. Pfeiffer, and K. W. West, "Mesoscopic structures and two-dimensional hole systems in fully field effect controlled heterostructures," *Appl. Phys. Lett.* **91**, 033510 (2007).
- 11 S. Sarkozy, K. Das Gupta, C. Siegert, A. Ghosh, M. Pepper, I. Farrer, H. E. Beere, D. A. Ritchie, and G. A. C. Jones, "Low temperature transport in undoped mesoscopic structures," *Appl. Phys. Lett.* **94**, 172105 (2009).
- 12 W. Pan, K. W. Baldwin, K. W. West, L. N. Pfeiffer, and D. C. Tsui, "Antilevitation of Landau levels in vanishing magnetic fields," *Phys. Rev. B* **94**, 161303 (2016).
- 13 W. Pan, W. Kang, K. W. Baldwin, K. W. West, L. N. Pfeiffer, and D. C. Tsui, "Berry phase and anomalous transport of the composite fermions at the half-filled Landau level," *Nat. Phys.* **13**, 1168–1172 (2017).
- 14 C. T. Harris and T.-M. Lu, "A PtNiGe resistance thermometer for cryogenic applications," *Rev. Sci. Instrum.* **92**, 054904 (2021).
- 15 S. F. Adam, *Microwave Theory and Applications* (Prentice Hall, 1969).
- 16 From Sonnet Software, Syracuse, NY, www.sonnetsoftware.com.
- 17 M. M. Fogler and D. A. Huse, "Dynamical response of a pinned two-dimensional Wigner crystal," *Phys. Rev. B* **62**, 7553–7570 (2000).
- 18 J. P. Eisenstein, L. N. Pfeiffer, and K. W. West, "Compressibility of the two-dimensional electron gas: Measurements of the zero-field exchange energy and fractional quantum Hall gap," *Phys. Rev. B* **50**, 1760–1778 (1994).
- 19 R. Mehrotra and A. J. Dahm, "Analysis of the Sommer technique for measurement of the mobility for charges in two dimensions," *J. Low Temp. Phys.* **67**, 115–121 (1987).
- 20 P. J. Burke, I. B. Spielman, J. P. Eisenstein, L. N. Pfeiffer, and K. W. West, "High frequency conductivity of the high-mobility two-dimensional electron gas," *Appl. Phys. Lett.* **76**, 745–747 (2000).
- 21 G. Ghione and C. U. Naldi, "Coplanar waveguides for MMIC applications: Effect of upper shielding, conductor backing, finite-extent ground planes, and line-to-line coupling," *IEEE Trans. Microwave Theory Tech.* **35**, 260–267 (1987).
- 22 See example <https://microwaves101.com/calculators/864-coplanar-waveguide-calculator>.
- 23 S. M. Sze, *Physics of Semiconductor Devices*, 2nd ed. (Wiley-Interscience, 1981), p. 849.
- 24 K. Seeger, *Semiconductor Physics: An Introduction*, 4th ed. (Springer, 1988), p. 63.